GOPEX Laser Transmission and Monitoring Systems

G. Okamoto and K. Masters
Communications Systems Research Section

This article describes the laser transmission and monitoring system for the Galileo Optical Experiment (GOPEX) at the Table Mountain Facility (TMF) in Wrightwood, California. The transmission system configuration and the data measurement techniques are described. The calibration procedure and the data analysis algorithm are also discussed. The mean and standard deviation of the laser energy transmitted each day of GOPEX show that the laser transmission system performed well and within the limit established in conjunction with the Galileo Project for experiment concurrence.

I. Introduction

The Galileo Optical Experiment (GOPEX) was conducted from December 9–16, 1992, when laser transmissions from the Table Mountain Facility (TMF) in Wrightwood, California, and the Starfire Optical Range (SOR) in Albuquerque, New Mexico, were successfully detected by the Galileo Solid State Imaging (SSI) camera [1]. The laser system at TMF was operated and maintained consistent with the Galileo Project's concurrence requirement of mean energy of 250 mJ, with a 10-percent margin. The laser was electronically controlled and monitored, and pulse output characteristics were recorded at both TMF and SOR. This article describes the laser-transmission-control and laser-emission monitoring systems at TMF. Section II discusses the laser equipment at TMF; Section III discusses the data measurement techniques; Section IV contains the results and analysis; and Section V contains the conclusion. Analysis of the data showed that the laser performed as expected and was maintained within the requirements.

II. Laser Equipment

Figure 1 shows the operational setup of the laser and optics system in the coudé path of the TMF 0.6-m telescope. The laser (labeled A in the figure) was a dual ellipse flashlamp-pumped neodymium: yttrium-aluminum-garnet (Nd:YAG) oscillator/amplifier with a second harmonic generator [2]. It can produce laser pulses at 12 nsec full-width half-maximum (FWHM), with 0.7-mrad beam divergence and repetition rates of 5, 6, 10, 15, and 30 Hz. The beam-steering mirrors (labeled B in the figure) were high-damage-threshold dielectric coated 2-in. fused silica. The coating was dielectric stack with a high reflection at 532 nm and a high transmission at 1064 nm for 45-deg incident radiation. The convex and concave lenses (labeled D and E in the figure) have an antireflecting coating for 532 nm. These lenses were used to control the beam divergence leaving the telescope (110 μrad for the case shown). The mirror (labeled B in the figure) and both lenses (labeled D and E) were moved to position 3, and both mirrors (labeled F) were removed for the 60-μrad

case, as noted by the dotted components and transmission path. The other beam-steering mirrors (labeled F) were high-damage-threshold dielectric coated 1-in. fused silica, coated for maximum reflection for 532 nm at near-normal incidence. A flip mirror (labeled H in the figure) was used to direct the light from the telescope into an eyepiece (labeled J in the figure) for viewing and aligning stars in the field-stop aperture (labeled G in the figure). The alignment was done only when the laser was off. The flip mirror (labeled K in the figure) was used to direct the laser beam into the camera (labeled P in the figure), which was connected to the Beam-code computer (labeled Q) in the figure. Beam-code is a beam-profile-analyst software and hardware setup from the Big Sky Software Company that was used to adjust and fine-tune the laser. It was also used to align the outgoing laser beam to the field-stop aperture. Detailed information about the optical setup is presented in [3] in this volume.

The GOPEX Monitoring Program recorded all the data presented in this article. The monitoring software was developed by the JPL Instrumentation Group to enable the user to control the Tektronix DSA 602A Digitizing Signal Analyzer. The software used LabWindows by National Instruments as the programming environment. This created an interactive graphical interface for the program. Configuration files were created so that the proper configuration could be loaded before each frame of data was to be taken. A total of 133 frames of usable data were recorded, with each frame containing 46 or 92 laser pulses, depending on the transmission duration. Each laser pulse waveform was stored in a separate file and each frame was stored on a different disk. Data from these disks were later archived to an optical disk for permanent storage.

III. Data Measurement

Because the GOPEX team needed to record both pulse width and energy of each laser pulse transmitted to Galileo, a fast detector with a rapid data acquisition and storage system was needed. The Hamamatsu R1193u photo detector combined with the Tektronix DSA 602A digital storage oscilloscope was used to rapidly record each outgoing laser pulse form. From these data both the pulse width (FWHM) and the energy per pulse calculated from the area under the pulse form were obtained.

The photodetector was positioned at position 1, as seen in Fig. 1. At this point the detector monitored the leakage through the turning mirror B_v. A 532-nm bandpass interference filter rejected the 1.06-laser light.

By measuring the reflected energy at position 2 (not shown in Fig. 1 because it was removed after calibration) using an Ophir power meter and comparing that with the integrated area measured by the DSA 602A, the energy per pulse transmitted to the spacecraft was deduced. Ten measurements were made at each of seven different laser power levels with the Hamamatsu at position 1 and the Ophir at position 2. Each set of Ophir power meter readings was averaged and recorded along with the corresponding integrated pulse area displayed by the DSA 602A. The results (shown in Fig. 2) are plotted for various laser power levels. To ensure that the laser beam characteristics (i.e., pulse shape and beam profile) were unchanged at the various power levels, the laser oscillator settings were held constant and the laser output energy was changed by detuning the delay time of the firing of the amplifier flash lamp away from its optimum setting.

All transmission data were recorded on floppy diskettes using the floppy drive in the DSA 602A. Each data file included a variable-length header of approximately 300 bytes in a text format followed by two-byte data points in a binary format. The header contains such information as the time and date the data were recorded, the waveform name and number, and the scope settings. The multiplier factors to convert the horizontal and vertical scales into physical units were computed from the information contained in the header, the information recorded on each night of transmission, and the specifications of the DSA 602A [4].

By using an IBM-compatible computer, data were extracted, scaled, and integrated to find the area of each laser pulse. The results were compared with the calibration data to translate the area computed into laser energy values. Measurements taken daily of the GOPEX transmission system using the power meter and the DSA 602A were used to validate these results.

The conversion factors needed to compute the energy of the laser pulses from the raw data values of the stored laser pulses were computed as follows: The interval of time between data points in seconds was computed, as were the proper scaling factors required to convert the raw data values into voltage readings. The time and voltage values were then used to compute the area of the laser pulses in units of picovolts squared times seconds (pVVsec) to be consistent with the units in which the calibration data were taken by the DSA 602A. The computed area value was translated into an energy value by using the conversion scale shown in Fig. 2 and linearly interpolating between the nearest two data points to find the appropriate scaling factor. The area was calculated as follows:

The interval of time between data points in seconds on the DSA 602A, x_{mult}, was calculated by dividing the time in the interval by the number of sample points in the interval using

$$x_{mult} = D_x(X/X_r) \tag{1}$$

where D_x is the number of horizontal divisions, X is the horizontal sensitivity of the oscilloscope set by the monitoring software in seconds, and X_r is the number of valid sample points recorded in the timing interval.

Data were digitized over a 64-K value range (R) and scaled into voltage values by y_{mult}, calculated by

$$y_{mult} = D_y(Y/R) \tag{2}$$

where D_y is the number of vertical divisions and Y is the vertical sensitivity of the oscilloscope set by the monitoring software in volts per division. The data values were then converted into volts (V) by

$$V = \text{data}(y_{mult}) \tag{3}$$

The area of the laser pulse was computed by multiplying the voltage squared of each sample point by the time interval of the sample point and then summing over all sample points. Using the calibration measurements, the area of the laser pulse was converted into energy, as shown in Fig. 2. The exact energy reading was then interpolated linearly between the nearest two data points in Fig. 2 to get the most appropriate scaling factor.

From these data, the mean laser output energy for each frame and day given by [5] is

$$\mu = \frac{1}{N}\sum_{i=1}^{N} E_i \tag{4}$$

where μ is the mean energy, E_i is the energy of the particular laser pulse, and N is the number of laser pulses in the desired frame or day. The variance (σ^2) of the set of laser pulses given by [5] is

$$\sigma^2 = \frac{1}{N-1}\sum_{i=1}^{N} (E_i - \mu)^2 \tag{5}$$

IV. Results and Analysis

Table 1 shows the mean and standard deviation for the output of the laser for each of the GOPEX days. No data were available for days 4 and 5 since TMF was shut down on day 4 due to weather and there were no planned GOPEX activities on day 5. Figure 3 shows a plot of the mean laser output for each day, and Figs. 4–9 plot the mean for each frame in each day, with the overall mean for the day noted by a dotted line. Certain frames on the first three days are not shown because no transmission took place due to U.S. Space Command prohibitions, weather problems, or equipment failures. The intensity fluctuations from pulse to pulse, as seen in Figs. 4–9, were expected since the transmission system used a flashlamp-pumped laser.

The mean laser energy for the first two days, as shown in Table 1, was significantly less than the other days because of the aging flashlamps in the laser system. The laser energy for the second day was approximately 20 percent lower than the first day because of a timing problem that was discovered and corrected after the second day of transmission. This reduction in energy resulted in a noticeable drop in the intensity level of the signals received at the spacecraft, much lower than the signal levels received from SOR for that day. The flashlamps were replaced before the third day of GOPEX. This boosted the laser power to the expected level (250 mJ). The laser power was increased slightly on the seventh day to compensate for the long transmission distance. The laser power was increased again on the eighth day for the same reason. On all days, the mean laser power remained within the 10-percent margin allowed by the experiment concurrence negotiated with the Galileo Project.

V. Conclusion

The GOPEX laser transmissions at TMF were successfully detected by the Galileo SSI camera. The output of the laser was monitored by a photodetector which sent the detected signal to a Tektronix DSA 602A Digitizing Signal Analyzer which, in turn, was controlled by the GOPEX monitoring system. The monitoring system then transferred the data to storage diskettes. Software was created to extract all the data and compute the mean and standard deviation for each frame of each day, as well as for each day overall. These results show that the GOPEX laser transmission system performed as expected and was maintained within specifications.

Acknowledgments

The authors gratefully acknowledge the support provided by J. McGregor, F. Loya, and E. Baroth of the Instrumentation Section's Measurement Technology Center at JPL. The authors would like to thank the staff at TMF for their excellent support. They also thank T.-Y. Yan of the Communications Systems Research Section at JPL for his helpful suggestions about this article.

References

[1] K. E. Wilson and J. R. Lesh, "An Overview of the Galileo Optical Experiment (GOPEX)," *The Telecommunications and Data Acquisition Progress Report 42-114, vol. April–June 1993*, Jet Propulsion Laboratory, Pasadena, California, pp. 192–204, August 15, 1993.

[2] *YG580 Operation and Maintenance Manual*, Santa Clara, California: Quantel International, 1986.

[3] J. Yu and M. Shao, "The Galileo Optical Experiment (GOPEX) Optical Train: Design and Validation at the Table Mountain Facility," *The Telecommunications and Data Acquisition Progress Report 42-114, vol. April–June 1993*, Jet Propulsion Laboratory, Pasadena, California, pp. 236–247, August 15, 1993.

[4] *The DSA 601A and DSA 602A Digitizing Signal Analyzers User Reference*, Beaverton, Oregon: Tektronix, February 1991.

[5] P. R. Bevington, *Data Reduction and Error Analysis for the Physical Sciences*, New York: McGraw-Hill, 1969.

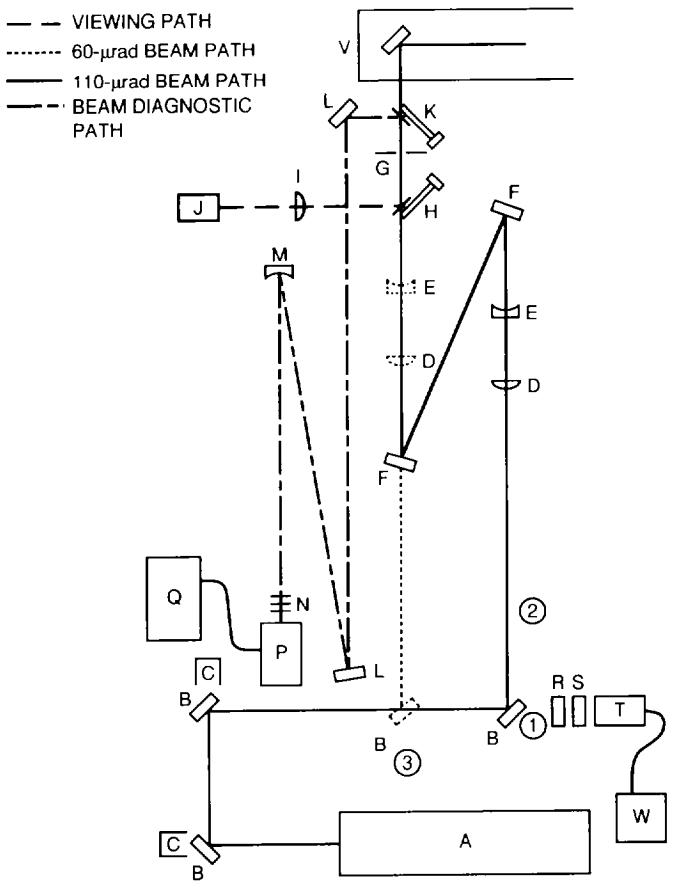

A. LASER CONTINUUM, yg581-30 w/SHG
B. MIRROR, R_{max} 532 nm
T_{max}, 1060 nm
C. LASER BEAM DUMP
D. CONVEX LENS
E. CONCAVE LENS
F. MIRROR, R_{max} 532 nm
G. FIELD STOP APERTURE
H. FLIP-IN FRONT SURFACE MIRROR
I. IMAGING LENS
J. EYEPIECE
K. FLIP-IN BARE GLASS
L. MIRROR, R_{max} 532 nm
M. MIRROR, 2 mcc R_{max} 532 nm
N. ND FILTERS
P. CAMERA
Q. BEAM-CODE COMPUTER
R. GROUND-GLASS DIFFUSER
S. 532-nm BANDPASS FILTER
T. PHOTODETECTOR
W. DSA 602A TEKTRONIX ANALYZER
V. 0.6-m TELESCOPE

1. ENERGY AND TRANSMITTED DIAGNOSTICS
2. TEMPORARY POSITION OF POWER METER FOR CALIBRATION
3. MIRROR POSITION FOR 60-μrad BEAM PATH

Fig. 1. Optics setup.

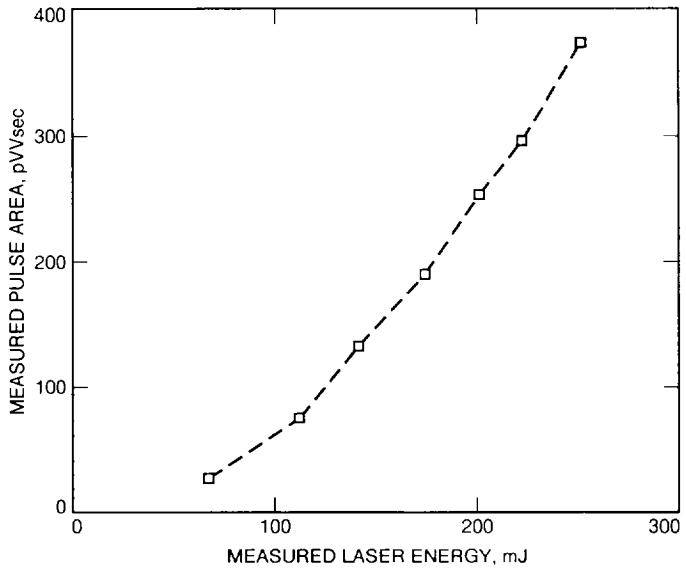

Fig. 2. Conversion curve for calibration data.

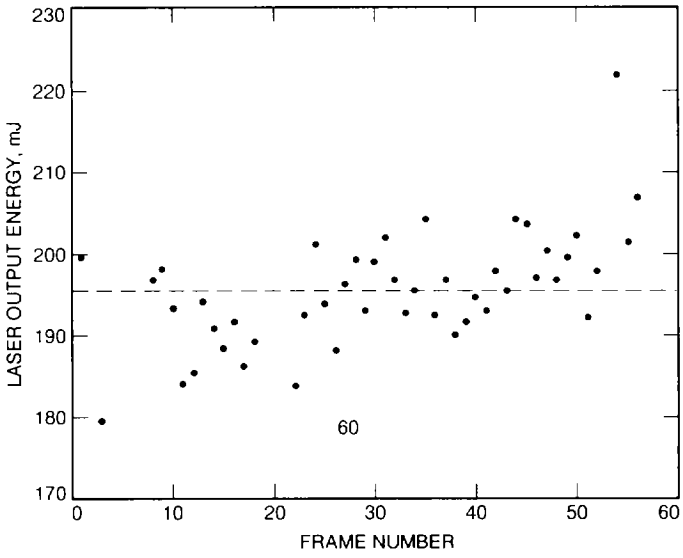

Fig. 4. GOPEX laser output for day 1.

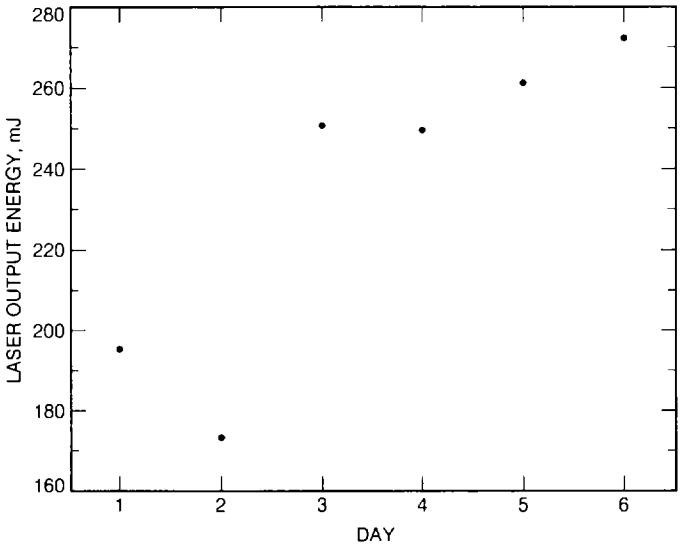

Fig. 3. GOPEX laser energy output per day.

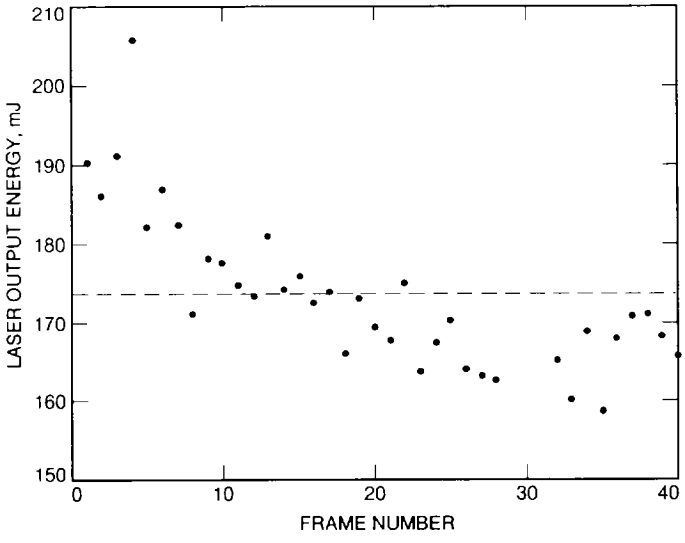

Fig. 5. GOPEX laser output for day 2.

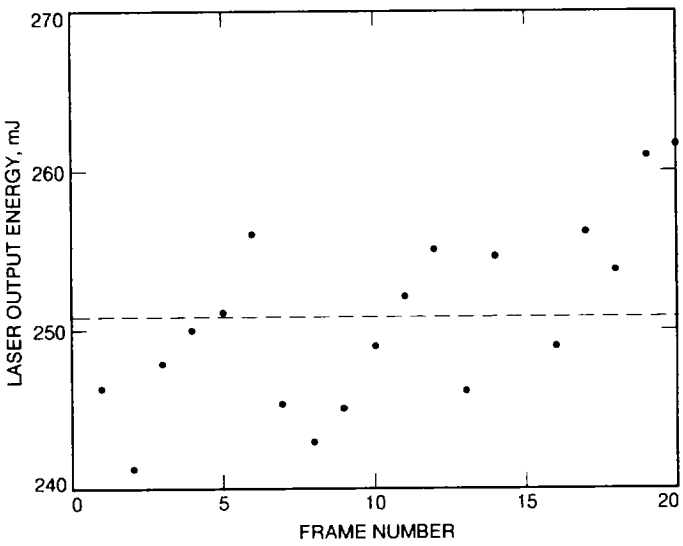

Fig. 6. GOPEX laser output for day 3.

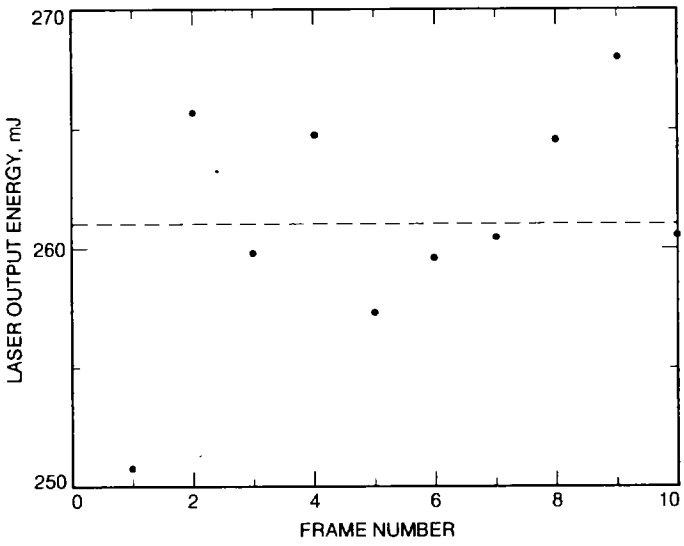

Fig. 8. GOPEX laser output for day 7.

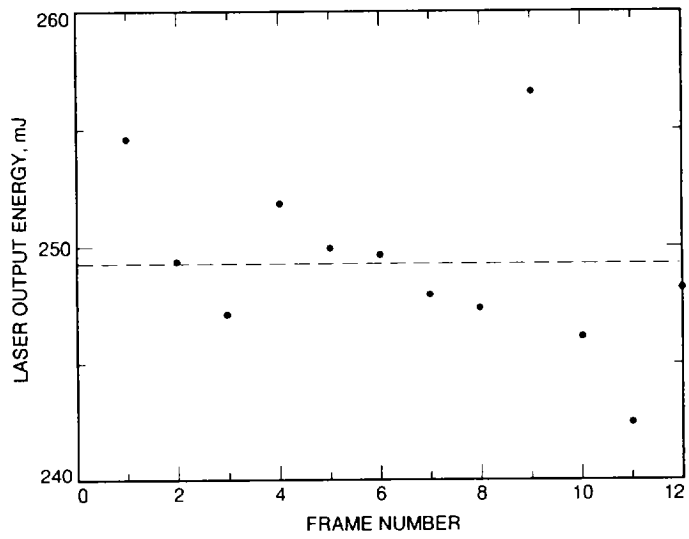

Fig. 7. GOPEX laser output for day 6.

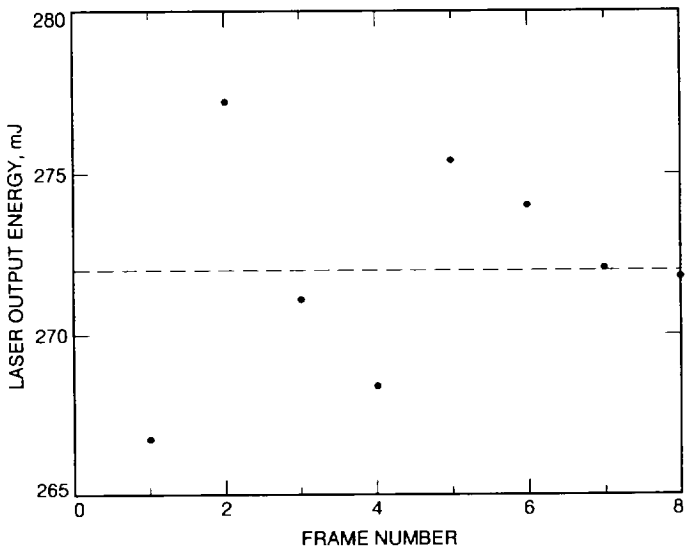

Fig. 9. GOPEX laser output for day 8.